KSME Journal, Vol. 8, No. 3, pp. 255~263, 1994

A New Tracking System for Magneto-Optical Disk Drives —Part I : Design

Kyihwan Park* and Ilene J. Busch-Vishniac**

(Received November 17, 1993)

To reduce the average accessing time of a magneto-optical(MO) disk drive, which is a severe drawback of current products, a newly developed moving-magnet type tracking actuator has been implemented and will be tested. The moving-magnet type actuator meets the following objectives which the known prior actuator designs have not been able to satisfy: providing sufficiently high magnetic force constants over essentially the whole stroke length of the actuator, achieving extremely rapid accessing time while providing a mechanically stiff carriage; eliminating the carriage thermal expansion which causes a head misalignment on disk tracks; eliminating flexible cable connections to the moving parts; providing a very compact design, and reducing the cost of manufacturing. Computer aided design using magnetic circuit theory is applied for determining optimal design parameters for the actuator.

1. Introduction

Magneto-optical disk(MO) is a memory device which reads and writes data optically using a magnetic field. Because the MO disk systems are erasable they are being increasingly used as computer external memory device. The MO disk has some advantages over the traditional magnetic floppy disk drive, namely, a higher capacity due to a high track density, and less susceptibility to mechanical wear because only the laser beam affects the surface of the magneto-optical disk. On the other hand, it has one significant disadvantage compared to magnetic system, namely, its slow accessing performance which results in a low data transfer rate. The relatively sluggish performance of MO drives derives from a few factors: The reading/writing mechnisms of MO drives need two degrees of actuation, which are tracking and focusing actuations, and they lead to a heavy actuator. Many optical components required for transmitting and receinving a laser beam also make the system heavy. As another factor, the small track pitch causes tracking difficulties. Note that all of the causes of slow accessing are related to the immaturity of magneto-optical recording systems. Lighter heads, improved actuators, and more powerful lasers will facilitate much faster magneto-optical disk systems. Currently the average accessing time, defined as the time to move 1/3 of a full stroke, in magneto-optical(MO) 5.25 inch disk systems is greater than 100 ms. By comparison, in magnetic disk systems, accessing times as low as 20 ms have been produced.

To enhance a understanding of the MO disk systems, a driving process of them is investigated. Two separate tracking servo mechanisms traditionally have been used in the tracking operation as a tandem coarse and fine positioner. In the tracking operation, the moving part or tracking actuator which has an objective lens and a focusing actuator is driven radially to the target track as shown in Fig. 1. It is first coarsely positioned to the vicinity of the target track with an accuracy of $\pm 1\ \mu m$. Next it is finely positioned by a fine positioner such as a galvano-mirror with an accuracy of $\pm 0.1\ \mu m$. In this tracking operation, most of the time is spent on coarse positioning. Therefore, it is necessary to develop a coarse positioner

*Department of Precision Engineering, Korea Advanced Inst. of Science and Technology, Taejon, 305-701, Korea.

**Department of Mechanical Engineering, The University of Texas at Austin, Austin, Texas 78712

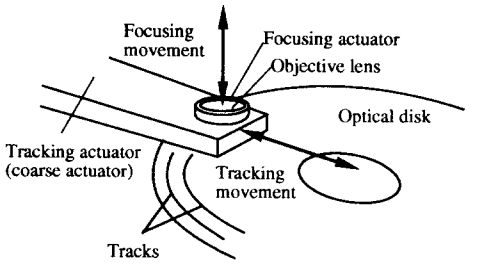

Fig. 1 Tracking actuator having an objective lens and a focusing actuator mounted is driven radially to the target track

which is capable of fast positioning and $\pm$ 1μm accuracy. This effort is the thrust of the research reported here.

All of the designs used in current products adopt moving-coil type actuator, where permanent magnets are fixed in a base frame while the electromagnets can move. However, the moving magnet type actuator, which has the opposite situation, has many advantages over the moving-coil type of actuator. First, the moving-magnet type actuator permits a compact (low mass) design of magneto-optical disk systems, which means higher acceleration for the same force.

Second, heat is generated by the coils in either actuator type, but it is easier for the moving-magnet type actuator to dissipate heat because the coils are stationary. Moreover, since the coils are part of the moving structure in a moving-coil actuator, the accuracy might degrade due to temeperature changes.

Third, the moving-magnet actuator requires no power source in its moving parts. Thus it can move freely while the moving-coil actuator requires the moving parts to be tethered to a power source.

Fourth, in the moving-magnet type actuator the cost of manufacturing is lower because the permanent magnets can be much smaller than the ones which are used in the moving-coil type actuator. The cost of permanent magnets scales roughly with their volume, and they represent a significant fraction of the material costs in magnetic systems.

In conclusion, the moving-magnet actuator is adopted for the development of magneto-optical disk driving actuator in this work because it offers a simple and compact design which produces high acceleration. This type of actuator is much less sensitive to temperature changes than the moving-coil type of actuator, which can serve to improve accuracy.

A new linear tracking actuator which theoretically can achieve less than a 25 ms accessing time at the required accuaracy for a 3.5 inch disk magneto-optical system is presented.

In Sec. 2, basic equations for developing the tracking actuator are derived. In Sec. 3, design of the tracking is introduced. Servo control system and experimental results in terms of speed and accuracy will be provided in Part 2.

2. Force Characteristics of an Air Core Solenoid and Permanent Magnet System

2.1 Analysis of forces in magnetic fields

For a point dipole moment **m** in a magnetic field **B**, the force that the magnetic dipole moment experiences can be derived by applying the Lorentz force law, and this is expressed in a vector form (Griffith, 1989).

$$\boldsymbol{F}=(\boldsymbol{m}\cdot\nabla)\boldsymbol{B}. \tag{1}$$

Also, the torque on the dipole is expressed (Pelrine, 1988)

$$\boldsymbol{T}=\boldsymbol{m}\times\boldsymbol{B}. \tag{2}$$

When a permanent magnet is in a steady state condition with z as the pole face axis and the axis pointing to the surface of an air-core coil (i.e. $m_x=m_y=0$), Eqs. (1) and (2) can be simplified to

$$F_x=m_z\frac{\partial B_x}{\partial z}, \tag{3}$$

$$F_y=m_z\frac{\partial B_y}{\partial z}, \tag{4}$$

$$Fz=m_z\frac{\partial B_z}{\partial z}, \tag{5}$$

$$T=-m_zB_y\boldsymbol{i}+m_zB_x\boldsymbol{j}, \tag{6}$$

where $\boldsymbol{i}$ and $\boldsymbol{j}$ are unit vectors in the x and y direcrtions respectively. Eqs. (3)~(6) will be used to compute the forces and torques experienced by permanent magnets in the tracking actuator developed here.

Solenoids and permanent magnets or electromagnets are used in pairs to produce a force tracking actuator. Air core coils have a few advantages over iron cores in that they have no hysteresis, no eddy current loss, and no saturation of flux density. These characteristics all serve to increase the accuracy which can be achieved. Permanent magnets are being used in many applications of small magnetic systems because they can supply a sufficient force and they are suitable for compact design. Hence for design of new tracking actuator, one would prefer using air core solenoids paried with permanent magnets.

Figure 2 shows the cross-section of a solenoid with a unit dipole moment suspended above it. In Fig. 2, A_o, R_o, n_o, m_o, d_w, and l_g indicate the inner radius, outer radius, number of layers, number of turns per layer, wire diameter and air gap between the permanent magnet and the solenoid respectively. In this and subsequent sections of this article we will examine the force characteristics of permanent magnets by considering the air core solenoid and point dipole.

There are two types of forces present in a permanent magnet / solenoid system: radial force, F_r and axial force, F_z. The general trends of those forces are drawn in Fig. 3. F_r has a constant value in a wide range. In addition, control can be accomplished easily because F_r is proportional to the supplied current. F_z has a maximum a little away from the surface of the solenoid and then decreases steeply. F_z is a function of both supplied current and displacement, and has a big force in a small range. From these results we choose F_r for the tracking actuator because a long range of tracking motion is required. Moreover, F_r provides a constant force characteristic.

2.2 Acceleration capability in the moving magnet type actuator

Let us investigate how much acceleration can be obtained in the moving-magnet actuator with the air core solenoid. Assuming a unit dipole moment for the permanent magnet, the radial force varies according to the coil geometry.

Figure 4 shows the force characteristics for different coil geometries. These results are obtained by assuming a 25 mg unit dipole moment, 0.5 mm wire diameter, 1 mm air gap, and 5 A of current. The number of turns per layer is fixed to 40. As the number of layers increases, the radial force, F_{5A}, increases; however, the range of constant force decreases as shown in Fig. 4. A

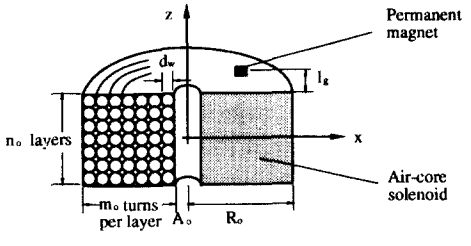

Fig. 2 Geometry of the air-core solenoid

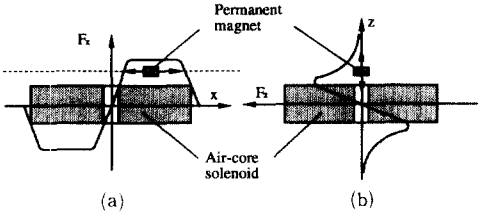

(a) In the radial direction
(b) In the axial direction

Fig. 3 Force characteristics in a solenoid

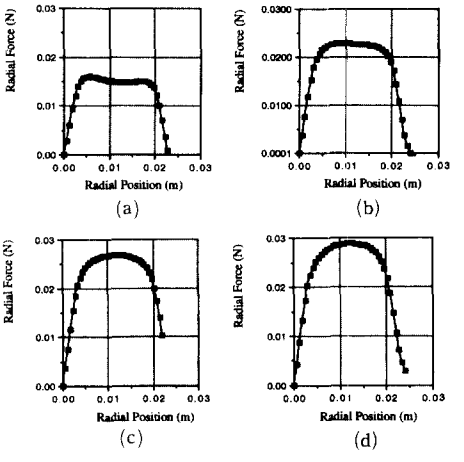

(a) 40 turns 10 layers (40×10)
(b) 40 turns 20 layers (40×20)
(c) 40 turns 30 layers (40×30)
(d) 40 turns 40 layers (40×40)

Fig. 4 Force characteristics for different coil geometries

wide range of high constant force is required for fast accessing over the necessary tracking distance. In Fig. 4, case (b) for example, provides a force of 23 mN with 25 mg of unit dipole moment. Thus, the acceleration a obtainable in this coil geometry when using 1 A is $a=F_{5A}/(5 \cdot mass)=184m/s^2 \approx 20$ g's.

If bang-bang control is used for a minimum time control, maximum acceleration will act untill the tracking actuator reaches half of the required displacement, at which point a maximum deceleration will act untill it stops on a target track in the allotted time t. Provided that the maximum acceleration is equal to the maximum deceleration, the average track seeking time, t_s, is expressed by

$$t_s=2\sqrt{\frac{x_{max}}{3a}}, \tag{7}$$

where x_{max} is a total moving stroke. But Eq. (7) does not include the settling time required for the tracking actuator to slide smoothly toward a target track. Hence, the average access time, t_{av} which includes the settling time can be expressed by

$$t_{av}=3\sqrt{\frac{x_{max}}{3a}}. \tag{8}$$

Here, the settling time is assumed to take the half of the access time (Hertrich, 1965). From Eq. (8), we can expect t_{av} to be as low as 17 ms for a 3.5 inch magneto-optical disk drive ($x_{max}=18$ mm) when the maximum acceleration is 184 m/s^2.

However, only the mass of the permanent magnet was considered in estimating the accessing time in Eq. (8). In reality, an additional mass is required due to the structure to which the magnets are attached, and this decreases the maximum acceleration. In this paper, this fact is reflected as setting the average accessing time to 25 ms.

The force required, F_r, to move the tracking actuator of mass m_a one third of the distance of a total stroke in an average accessing time is

$$F_r=\frac{4m_a x_{max}}{3t_{av}^2}. \tag{9}$$

Since Eq. (9) neglects factors such as current rise time, friction and settling time due to inefficient control, it is appropriate to apply a correction-factor of about 2 (Oswald, 1981) to the result. If there is a time delay in an electric circuit characterized by a time constant t_e, the pure time available for acceleration can be considered as $(t_{av}-t_e)$. Therefore, the compensated and delay-corrected required force is

$$F_r=\frac{2.67m_a x_{max}}{(t_{av}-t_e)^2}. \tag{10}$$

Provided that t_e is small enough to be negligible, which is dependent on the quality of the current source, the force required for 25 ms accessing time in a 3.5 inch magneto-optical disk drive, for example, is $85.4m_a$. When m_a is 20 g, $F_r=1.7$ N.

To estimate how much mass of permanent magnets is required for producing $F_r=1.7$ N, we refer to Fig. 4(b). 9.25 gr of permanent magnets' mass is expected for 1 A.

3. Design of the Tracking Actuator

3.1 Design concept

From the previous analysis, we can anticipate the performance of system of magnets and solenoids. A good candidate design for the magneto-optical tracking actuator is shown in Fig. 5. If four magnets are arranged with magnetic dipole moment orientations as shown in Fig. 5(a), we have four times as much force as when only one magnet is used. This arrangement also cancels unfavorable forces and torques, thus reducing the friction between the magnets and the structure. The four magnets are driven simultaneously by the same current. The geometry of the magnets and solenoid are described in Fig. 5(b).

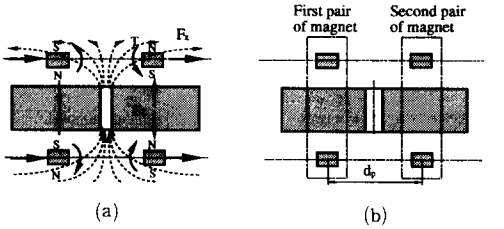

Fig. 5 (a) Forces and torques acting on four magnets hanging above and below a solenoid with different magnet dipole moments
(b) The geometry of the tracking actuator

In order to progress further on the design, it is necessary to remove the assumption of a unit dipole moment by introducing the parameters of real permanent magnets. As Eqs. (3)~(6) indicate, the dipole moment of the permanent magnet is the most important parameter, and the higher the moment, the higher the generated forces and torques. Rare-earth magnets are an advanced group of recently developed magnetic materials which combine high remanence with high coercivity. Among the rare-earth magnets, neodymium-iron-boron(NdFeB) magnets are far less subject to cracking and chipping than samarium-coblat (SmCo) magnets while having lower specific gravity. Hence, NdFeB magnets are suitable for the moving-magnet type actuator which requries small and light moving parts. The magnetization of the NdFeB magnet M, residual remanence ϕ_{ro}, coercivity $\Im_o$, and specific gravity used for this work, are 0.00309 A/m, 1.15 T, 867.6 KA/m, and 7.4 respectively.

Having chosen the permanent magnet material, we can use Eqs. (3) through (6) to determine the dimension of the air core solenoid and permanent magnets needed for the actuating force, but this process of force evaluation requires much computation. A small change in the design parameters requries a new iteration of the entire process. As an alternative rigorous numerical solution, we used magnetic circuit theory as a tool for developing a simplified mathematical model based on lumped discrete elements rather than continuum elements (Park, 1993). We used the model to determine reasonable parameters for the magnet and solenoid dimensions, and then measured the force produced in the resulting design.

3.2 Magnetic circuit design

A magnetic circuit is analogous to an electric circuit except that voltage and current are replaced by magnetomotive force and magnetic flux respectively. Flux paths are modeled as magnetic reluctances or permeances which are functions of material properties and geometry. Permanent magnets can be modeled as constant magnetic flux sources or constant magnetomotive force sources.

There are three expressions that are used frequently to model magnetic fields. The first relates the magnetic flux to flux density:

$$\phi = \oint \boldsymbol{B} \cdot d\boldsymbol{A} \tag{11}$$

where $\boldsymbol{B}$ is the flux density in *Tesla*(*Webers*/m^2) and $\boldsymbol{A}$ is the cross-sectional area in square meters. This equation simply states that the total flux is the sum of the flux density components normal to the area through which the flux passes. The second equation relates the flux density, $\boldsymbol{B}$, to the magnetizing force, $\boldsymbol{H}$:

$$\boldsymbol{B} = \mu \boldsymbol{H} = \mu_o \mu_r \boldsymbol{H} \tag{12}$$

where $\boldsymbol{H}$ is in *amperes per meter* and μ is the permeability of the material. For convenience, μ is taken as the product of two components: the permeability of the free space, μ_o, and the relative permeability of the material, μ_r. The third expression relates the magnetomotive force, $\Im$, to the magnetizing force:

$$\Im = Ni = \oint \boldsymbol{H} \cdot d\boldsymbol{l}. \tag{13}$$

Since the magnetomotive force is analogous to the voltage, the ratio of *mmf* to flux is analogous to the inverse of capacitance in a *dc* circuit and is called the reluctance of the magnetic circuit. That is,

$$\Re = \frac{\Im}{\phi}. \tag{14}$$

Sometimes it is convenient to use permeance which is the reciprocal of reluctance in representing the magnetic flux paths because the permeance is directly analogous to electrical capacitance.

Because there are no fixed magnetic flux paths in the moving-magnet actuator, we need to assume that the magnetic flux flows in an imaginary control volume so that the permeances can be represented in terms of corresponding geometry and material properties. The permeances outside of the control volume are assumed to contribute little to the force in an air gap. This is justified becuase the permeances outside of the control volume have much smaller values than do the permeances inside of the control volume. Another assumption to be made is that the magnetic flux density in an air gap is locally uniform. These assumptions can result in an inaccurate absolute force evaluation, but the magnetic circuit theory

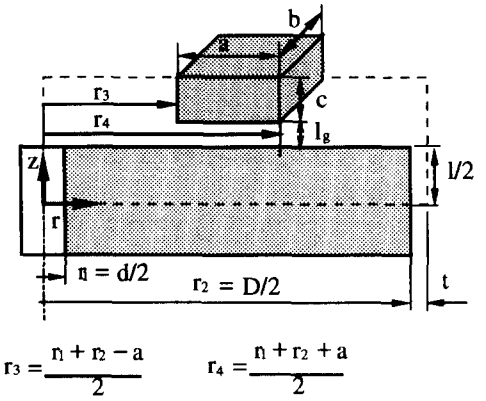

Fig. 6 Dimensions of magnetic circuit in a control volume

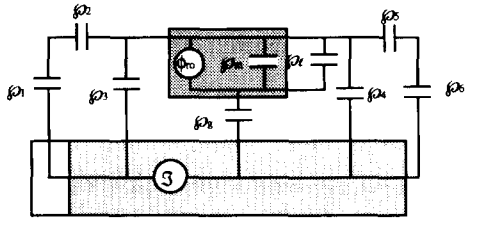

Fig. 7 Magnetic circuit model for the moving-magnet type tracking actuator

still can be used to establish a *relative comparison superiority* among magnetic systems.

Now lets's apply magnetic circuit theory to our proposed design as shown in Fig. 6. The symmetric configuration of the magnetic circuit allows us to model only one magnet and coil with the dimensions described in Fig. 6. In this figure, the inner diameter and the outer diameter of the air-core solenoid are indicated by d and D. The permanent magnet's width, depth and height are indicated by a, b, and c, respectively. The air gap is indicated by l_g. Fig. 7 represents a corresponding magnetic circuit.

We have constructed a magnetic circuit model that contains all design information through the following steps.

(1) Circuit topology:

$\mathcal{H}_1$: Permeance of air-core.

$\mathcal{H}_2$: Permeance of air, from $r=r_1$ to $r=r_3$.

$\mathcal{H}_3$: Permeance of air, from $z=c+l_g$ to $z=l_g$, for $r_1<r<r_3$.

$\mathcal{H}_4$: Permeance of air, from $z=c+l_g$ to $z=l_g$, for $r_4<r<r_2$.

$\mathcal{H}_5$: Permeance of air, from $r=r_4$ to $r=r_2$.

$\mathcal{H}_6$: Permeance of air, from $z=c+l_g$ to $z=0$.

$\mathcal{H}_g$: Airgap permeance.

ϕ_{ro} : Permanent nagnet flux source.

$\mathcal{H}_m$: Permanent magnet permeance.

$\mathcal{H}_l$: Permanent magnet leakage.

(2) Calculate permeances:

All permeances can be determined like below.

$$\mathcal{H}_1=\frac{\pi\mu_o r_1^2}{l} \tag{15}$$

$$\mathcal{H}_2=\frac{\pi\mu_o(c+l_g)}{\int_{r_1}^{r_2} dr/r}=\frac{\pi\mu_o(c+l_g)}{ln((r_1+r_2-a)/(2r_1))} \tag{16}$$

$$\mathcal{H}_3=\frac{0.5\pi\mu_o([(r_1+r_2-a)2]^2-r_1^2)}{l_g} \tag{17}$$

$$\mathcal{H}_4=\frac{0.5\pi\mu_o(-[(r_1+r_2+a)2])^2+r_1^2)}{l_g} \tag{18}$$

$$\mathcal{H}_5=\frac{\pi\mu_o(c+l_g)}{\int_{r_4}^{r_2} dr/r}=\frac{\pi\mu_o(c+l_g)}{ln(2r_2/(r_1+r_2+a))} \tag{19}$$

$$\mathcal{H}_6=\frac{2\pi\mu_o r_2 t}{l} \tag{20}$$

$$\mathcal{H}_g=0.5\frac{\mu_o ab}{l_g} \tag{21}$$

$$\phi_{ro}=abB_r \tag{22}$$

$$\mathcal{H}_m=\frac{\phi_{ro}}{\Im_{co}}=\frac{abB_r}{cH_c} \tag{23}$$

$$\mathcal{H}_l=\frac{4\mu_o(a+b)}{\pi}. \tag{24}$$

(3) Calculate an average flux density and force:

Figure 8 shows a simplified circuit model of the system, where

$$\mathcal{H}_{eq1}=\frac{\mathcal{H}_{13}\mathcal{H}_2}{\mathcal{H}_{13}+\mathcal{H}_2} \tag{25}$$

$$\mathcal{H}_{eq2}=\frac{\mathcal{H}_{46}\mathcal{H}_5}{\mathcal{H}_{46}+\mathcal{H}_5} \tag{26}$$

$$\mathcal{H}_{eq}=\mathcal{H}_{eq1}+\mathcal{H}_{eq2} \tag{27}$$

$$\mathcal{H}_{13}=\mathcal{H}_1+\mathcal{H}_3 \tag{28}$$

$$\mathcal{H}_{46}=\mathcal{H}_4+\mathcal{H}_6. \tag{29}$$

Defining $\mathcal{H}_{ml}=\mathcal{H}_m+\mathcal{H}_l$ for simplicity and applying nodal analysis to the simplified circuit we have two equations:

$$\phi_{ro}+\mathcal{H}_{ml}(\Im_2-\Im_1)=\mathcal{H}_g\Im_1 \tag{30}$$

$$\mathcal{H}_{eq1}Ni=\mathcal{H}_{eq}\Im_2+\phi_{ro}+\mathcal{H}_{ml}(\Im_2-\Im_1). \tag{31}$$

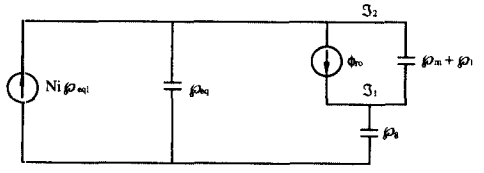

Fig. 8 Simplified circuit model for the moving-magnet type tracking actuator

Solving the above equations for $\mathfrak{H}_1$, we have

$$\mathfrak{H}_1=\frac{\phi_{ro}\mathfrak{H}_{eq}+\mathfrak{H}_{ml}\mathfrak{H}_{eq1}Ni}{\mathfrak{H}_g\mathfrak{H}_{eq}+\mathfrak{H}_g\mathfrak{H}_{ml}+\mathfrak{H}_{ml}\mathfrak{H}_{eq}}. \tag{32}$$

The magnetic flux in an air gap, ϕ_g, is $\mathfrak{H}_g\mathfrak{I}_1$. The average flux density, B_g is

$$B_g=\frac{\phi_g}{ab}=\frac{\mathfrak{H}_g(\phi_{ro}\mathfrak{H}_{eq}+\mathfrak{H}_{ml}\mathfrak{H}_{eq1}Ni)}{ab(\mathfrak{H}_g\mathfrak{H}_{eq}+\mathfrak{H}_g\mathfrak{H}_{ml}+\mathfrak{H}_{ml}\mathfrak{H}_{eq})}. \tag{33}$$

Finally, the force F can be calculated by using the *Lorentz force* relation

$$F=N_{eff}B_g il \tag{34}$$

where N_{eff} is the effective number of turns in the solenoid and l is an average coil length across which the magnetic flux passes.

3.3 Parametric design of the tracking actuator

The effects of each of the solenoid parameters on the radial force can be investigated using the simplified mathematical model because all the design information is included. First, let's investigate the force variation with respect to a permanent magnet's geometry when the permanent magnet's volume, V_{mag}, is kept constant and other design parameters have the following designated values.

$$l_g=1\text{mm},\ r_1=2\text{mm},\quad r_2=24\text{mm},\ l=11\text{mm}. \tag{35}$$

If we set

$$V_{mag}=abc=300[\text{mm}^3] \tag{36}$$

and define

$$a_n=\frac{a}{a_m},\ b_n=\frac{b}{b_m},\ F_n=\frac{F}{F_m} \tag{37}$$

then, the normalized force, F_n becomes a function of both a_n and b_n, where a_m and b_m are maximum

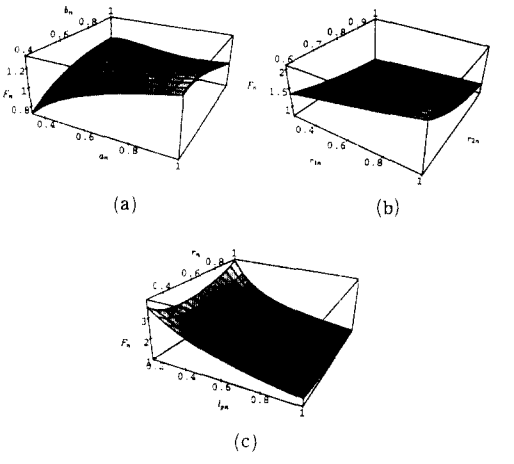

Fig. 9 (a) Force variation with respect to the permanent magnet geometry
(b) Force variation with respect to the coil geometry
(c) Force variation with respect to an air gap along the radial distance

magnet dimensions, and these are chosen as 14 mm and 17 mm. F_m is the force at $a=a_m$ and $b=b_m$ and this is 2.1 on the normalized scale. The force variation with respect to the permanent magnet geometry is described in Fig. 9(a).

Second, let's investigate the force variation with respect to coil geometry when the coil volume, V_{coil} is kept constant, and other design parameters have designated values,

$$a=6\text{ mm},\ b=12\text{ mm},\quad c=4\text{ mm},\ l=11\text{ mm}. \tag{38}$$

If we set

$$V_{coil}=\pi(r_2^2-r_1^2)\,l=2\times10^4[\text{mm}^3] \tag{39}$$

and define

$$r_{1n}=\frac{r_1}{r_{1m}},\ r_{2n}=\frac{r_2}{r_{2m}},\ F_n=\frac{F}{F_m} \tag{40}$$

then, the normalized force, F_n becomes function of only r_{1n} and r_{2n}, where r_{1m} and r_{2m} are the maximum dimensions of r_1 and r_2, and these are chosen as 4 mm and 28 mm respectively. F_m is the force at $r_1=r_{1m}$ and $r_2=r_{2m}$, and this is 1.6 on the normalized scale. The force variation with respect to the coil geometry is described in Fig. 9(b).

Third, let's investigate the force variation with

respect to the air gap l_g along the radial distance r when other design parameters have the following designated values.

$$a=6\text{ mm},\ b=12\text{ mm},\ c=4\text{ mm},$$
$$l=11\text{ mm},\ r_1=2\text{ mm},\ r_2=24\text{ mm} \quad (41)$$

and define

$$r_n=\frac{r}{r_m},\ l_{gn}=\frac{l_g}{l_{gm}},\ F_n=\frac{F}{F_m} \quad (42)$$

Then, the normalized force, F_n becomes function of only r_n and l_{gn}, where r_m and l_{gm} are maximum dimensions of r and l_g, and these are chosen as 24 mm and 5 mm, respectively. F_m is a force at $r=r_m$ and $l_g=l_{gm}$, and this is 0.55 on the normalized scale. r_m is set to r_{2m}. The force variation is described in Fig. 9(c).

From the magnetic circuit theory applied to the moving-magnet type of actuator, we can determine, therefore, that the most important design parameters are the permanent magnet geometry and air gap size. Thus, a magnetic circuit for the tracking actuator should be designed so that the permanent magnets stay as close to the surface of the coil as possible. The coil outer radius, r_2, will be determined by the total actuating stroke required for the tracking actuator to move over the data region in an optical disk. The coil inner radius has some freedom in its determination because it has little influence on the force.

Based on the pemanent magnets' mass requirement and results of the application of magnetic circuit theory, the magnets chosen for the tracking actuator have the dimensions of $a=6$ mm, $b=12$ mm, $c=4$ mm, and the air core solenoid for a 3. 5 inch disk drive has the dimensions of $d=4$ mm, $D=48$ mm, $l=12$ mm, and $N=1370$. If represented as normalized parameters, $a_n=0.42$, $b_n=0.71$. From Fig. 9(a), we predict that the force exerted with these design parameters is about 2 N using 1 A, which meets the force requirement to achieve 25 ms accessing time. the actual froce exerted from this magnetic circuit desgin needs to be verified by an experiment because the value from the magnetic circuit theory may not be accurate.

To investigate the static characteristics of the tracking actuator, Fig. 10 shows an experimental result for the force distribution as a function of radial distance with a current of 0.5A when two permanent magnets are arranged above and below the coil and facing each other. Here, we predict that the force exerted is about 1.8 N using 1 A. From the results obtained with magnetic circuit theory and the experiment, we can conclude that the forces are almost alike to each other.

To increase the force, two other magnets are placed a distance, d_p, from this permanent magnet pair on the opposite side of the core(see Fig. 5(a)). The force which results from the experiment using only one permanent magnet pair can be described in a closed form by employing a curve-fitting technique. Then the symmetric placement of the second pair of the magnets allows us to find the force for the entire magnet/solenoid system assuming no interaction between the pairs of magnets. The distance between the pairs of magnets, d_p, can be chosen by iteration so that the net force is high and constant over a wide range. Using this approach,the magnetic circuit shown in Fig. 5 was designed to exert 0.8 N for 0.5 A. With this, the proposed tracking actuator is capable of exerting a force of 1.6 N for a current of 1 A, and the force constant K_t, which is defined as a ratio of the force per unit current, is 1.6 N/A. We also can predict that a current of 1.1 A is

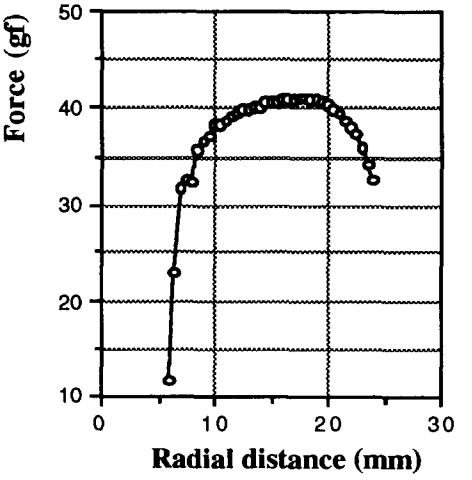

Fig. 10 Force distribution of tracking actuator over the radial distance

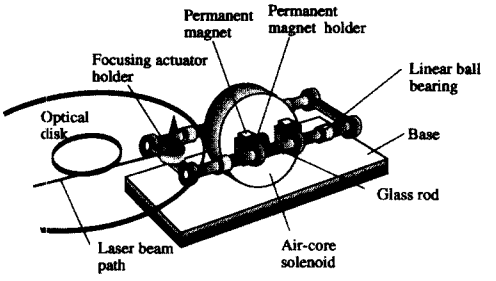

Fig. 11 Configuration of the developed linear tracking actuator

Table 1 The specifications of the tracking actuator.

	Product design
Coil resistance	16.5 Ω
Number of turns	1370(50 turns×27 layers)
Mass of permanent magnets	10g
Mass of actuator	22g
Force constant	1.6 N/A
Power consumption per unit current	17 W

required for exerting the necessary force to achieve 25 ms accessing time. The force constant will be used as a system gain in control of the tracking system.

Figure 11 shows the final design of the linear tracking actuator to be used in the magneto-optical disk drive. To reduce the mass of the actuator, two glass bars are used as the structure to which the magnets are attached. The shafts are connected together at both ends to increase the structural stiffness. The system specifications, all of which are design parameters or directly calculable from them, are given in Table 1.

4. Conclusion

A new actuating mechanism for magneto-optical disk drive systems which reduces the track accessing time has been desgined. A moving-magnet type of actuator is adopted for this work because it offers a simple and compact design of magneto-optical disk systems yet produces high acceleration. In addition, this type of actuator is much less sensitive to temperature changes than the moving-coil type of actuator, so accuracy can be improved.

A linear tracking actuator which uses a high power drive mechanism and has a stiff structure have been implemented. The dimensions of the permanent magnets and air core solenoid are determined by magnetic circuit theory so that a high and uniform force can be obtained in the moving range. The force constant of the developed tracking actuator is 1.6 N/A. With this value, a current of 1.1 A is expected to exert to achieve 25 ms accessing time.

References

Hertrich, F. R., 1965, "Average Motion Times of Positioners in Random Access Devices," *IBM Journal*.

Kyihwan Park., 1993, "Development of Tracking and Focusing Actuators for Magneto-Optical Disk Drive," Ph. D. *Dissertation*, Mechanical Engineering Department, University of Texas at Austin.

Marchant, A. B., 1990, *Optical Recording, A Technical Overview*, Addison-Wesley Publishing Company, Menlo Park, California.

Oswald, R. K., 1974, "Design of a Disk File Head-Positioning Servo," *IBM J. Res. Development*, 1974, pp. 506~512.

Oswald, R. K., Wasson, K. and Wagner, J. A., 1981, "The Disk File Linear Actuator: An Introduction to the Magnetics and Control," San Jose State University Engineering Institue.

Pelrine, R. E., 1988, "Magnetically Levitated Micro-Robotics," Ph. D. *Dissertation*, Mechanical Engineering Department, University of Texas at Austin.

Wangsness, R. K., 1979, *Electromagnetic Fields*, John Wiley & Sons, Newyork.